Surface & Coatings Technology 328 (2017) 115–120

Contents lists available at ScienceDirect

Surface & Coatings Technology

journal homepage: www.elsevier.com/locate/surfcoat

Mass-producible hydrophobic perfluoroalkoxy/nano-silver coatings by suspension flame spraying for antifouling and drag reduction applications

Mengjiao Zhai [a,b], Yongfeng Gong [a], Xiuyong Chen [a,*], Tonghu Xiao [b], Guoping Zhang [c], Lianghao Xu [c], Hua Li [a,*]

[a] Key Laboratory of Marine Materials and Related Technologies, Key Laboratory of Marine Materials and Protective Technologies of Zhejiang Province, Ningbo Institute of Materials Technology and Engineering, Chinese Academy of Sciences, Ningbo 315201, China
[b] Faculty of Materials Science and Chemical Engineering, Ningbo University, Ningbo 315211, Zhejiang, China
[c] China Ship Scientific Research Center, Wuxi 214082, China

ARTICLE INFO

Article history:
Received 21 June 2017
Revised 4 August 2017
Accepted in revised form 21 August 2017
Available online 23 August 2017

Keywords:
Suspension flame spraying
Hydrophobicity
Marine coatings
Antifouling
Drag reduction

ABSTRACT

To exploit marine metal materials with antifouling and drag reduction properties, we constructed hydrophobic perfluoroalkoxy (PFA)/nano silver (Ag) coatings onto aluminum substrates by suspension flame spray deposition of PFA/$AgNO_3$ composites. Silver nanoparticles were formed in situ within PFA coating during the suspension flame spraying. The successful construction of PFA/nano-Ag coatings was revealed by field-emission scanning electron microscopy (FE-SEM), X-ray diffraction (XRD), Fourier transform infrared spectroscopy (FTIR) and contact angle measurements, respectively. The additional silver nanoparticles play the significant role in regulating the sliding angle of the PFA-based coatings. The silver nanoparticles-loaded hydrophobic PFA coatings synergistically inhibited the adhesion of bacteria, while only PFA coatings with lower content of silver display drag reduction property. The simple and cost-effective approach is of great promise in mass-production of antifoulant-loaded hydrophobic coatings on general substrates for potential antifouling and drag reduction applications.

1. Introduction

Antifouling and low drag surfaces are two key issues of marine vehicles [1–3]. The settlement of marine fouling on the marine vehicles causes drag-related speed loss and increased fuel consumption [4–9]. During the past decades numerous research efforts have been devoted to investigating mechanism and application technologies of antifouling and drag reduction [10–14]. However, only a few reports have been published on the combine effect of antifouling and drag reduction [3, 15].

Recently, hydrophobic surfaces have drawn much attention as a new route for antifouling and drag reduction. For instance, the antifouling and drag reduction of hydrophobic surfaces in seawater was reviewed by Ferrari et al. [16]. The rice leaf and butterfly wing effect have been reported to develop novel hydrophobic surfaces for antifouling and drag reduction applications, as reviewed by Bixler et al. [17]. Many processing techniques have been attempted to fabricate hydrophobic surfaces [18]. However, most of these strategies still have difficulty in mass-production of hydrophobic surfaces. To overcome the aforementioned limitations of bioinspired hydrophobic surfaces, previously, we successfully fabricated hydrophobic coatings by suspension thermal spray [19, 20]. This approach can be used to fabricate hydrophobic coatings on general substrates with arbitrary shapes and sizes. To the best of our knowledge, there is no report describing the suspension thermal sprayed hydrophobic coatings for antifouling and drag reduction simultaneously.

Except for hydrophobic surfaces, the incorporation of antifoulant was also proved to be an efficient approach to impose antifouling property on marine surfaces [21], leading to low drag surfaces. It is well known that heavy metals, such as copper and silver, have strong antifouling effect towards a broad range of marine fouling. The antifouling mechanism of heavy metals was believed that metals ions adhered to the cell walls of marine fouling organisms, causing disruption of the permeability and organism death [22].

We hypothesized that hydrophobic coatings with antifoulant-loaded could inhibit the adhesion of biofouling and possess good drag reduction properties simultaneously. To confirm the hypothesis, aluminum substrates with polyfluoroalkoxy (PFA) coating and silver-loaded PFA coating were fabricated by suspension flame spraying and the synergetic effect of hydrophobicity and antifoulant of the PFA-based composite coatings on the regulation of antifouling and drag reduction properties were investigated.

* Corresponding authors.
E-mail addresses: chenxiuyong@nimte.ac.cn (X. Chen), lihua@nimte.ac.cn (H. Li).

http://dx.doi.org/10.1016/j.surfcoat.2017.08.049
0257-8972/

2. Experimental part

Aluminum plates (20 mm × 25 mm × 2.5 mm and 200 mm × 300 mm × 11.2 mm) were employed as substrates. Polyfluoroalkoxy with the size range of + 30–100 μm (PFA, Shenzhen Taotao Suhua Co. Ltd., China) was used for facilitating the hydrophobicity. PFA-based coatings were deposited by suspension flame spray (Wuhan Research Institute of Materials Protection, China) [19]. In this study, silver was chosen as a typical antifoulant, due to its strong antibacterial effect [23–25]. For PFA-based suspension preparation, PFA powder with a concentration of 5.0 wt% was added into ethanol solution and the suspension with sliver nitrate ($AgNO_3$, Aladdin Chemistry Co. Ltd., China) concentration of 0 wt%, 1.0 wt% and 10.0 wt% were explored, respectively. The as-sprayed coatings were designated as PFA coating, PFA/1%Ag coating and PFA/10%Ag coating, respectively.

Field emission scanning electron microscopy (FESEM, FEI Quanta FEG250, the Netherlands) was used for microstructure characterization of the coatings. Phases of the samples were evaluated by X-ray diffraction (XRD, Bruker AXS, Germany). Chemical composition of the samples was examined using Fourier transform infrared spectroscopy (FTIR, model 6300, Bio-Rad Co. Ltd., USA). Water static contact angle (CA) and sliding angle (SA) measurements were characterized using a video-based optical system (Dataphysics OCA20, Germany) by measuring five points for each sample. The water droplet size was 5 μL for CA measurement and 15 μL for SA measurement.

To investigate the release behavior of silver ions from the silver nanoparticles-loaded PFA coatings, PFA/1%Ag coating and PFA/10%Ag coating were immersed into a 6-well plate containing 7 mL sodium chloride (NaCl) solution in each well at room temperature for 7 and 21 days. The cumulative release of silver was monitored using an inductively coupled plasma optical emission spectrometer (ICP-OES, PE Optima 2100DV, Perkin-Elmer, USA).

Gram-negative *Escherichia coli* (*E. coli*), which was extensively studied for marine environment [26–33], were employed as the simplified model to evaluate the antifouling property of the samples in this study. *E. coli* were cultured in LB media (1.0% of NaCl, 0.5% of yeast extract and 1.0% of tryptone) shaken at 37 °C for 24 h. The *E. coli* suspension with an initial concentration of 10^6 cells/mL was prepared in artificial seawater (ASW). The samples were washed with ASW for three times after incubated for 24 h. For FESEM observation, the samples were fixed by 2.5% glutaraldehyde for 2 h and dehydrated by critical point drying using a graded series of ethanol.

Drag reduction tests were performed in cavitation tunnel system (China Ship Scientific Research Center, China). The flow velocity in test section is adjustable between 0 and 25 m/s. The flow velocities with 5, 8 and 11 m/s were chosen in this study. To comparatively investigate the influence of the coatings on drag, aluminum substrates, PFA coatings, PFA/1%Ag coatings and PFA/10%Ag coatings were systematically performed. Drag coefficients (C_f) were calculated according to the equation:

$$C_f = \frac{Z}{0.5\rho V^2 A}$$

where Z is the resistance of the samples; ρ is the density of water; V is the flow velocity in test section; and A is the projected area of the samples. Each measurement was performed for three times. Drag reduction

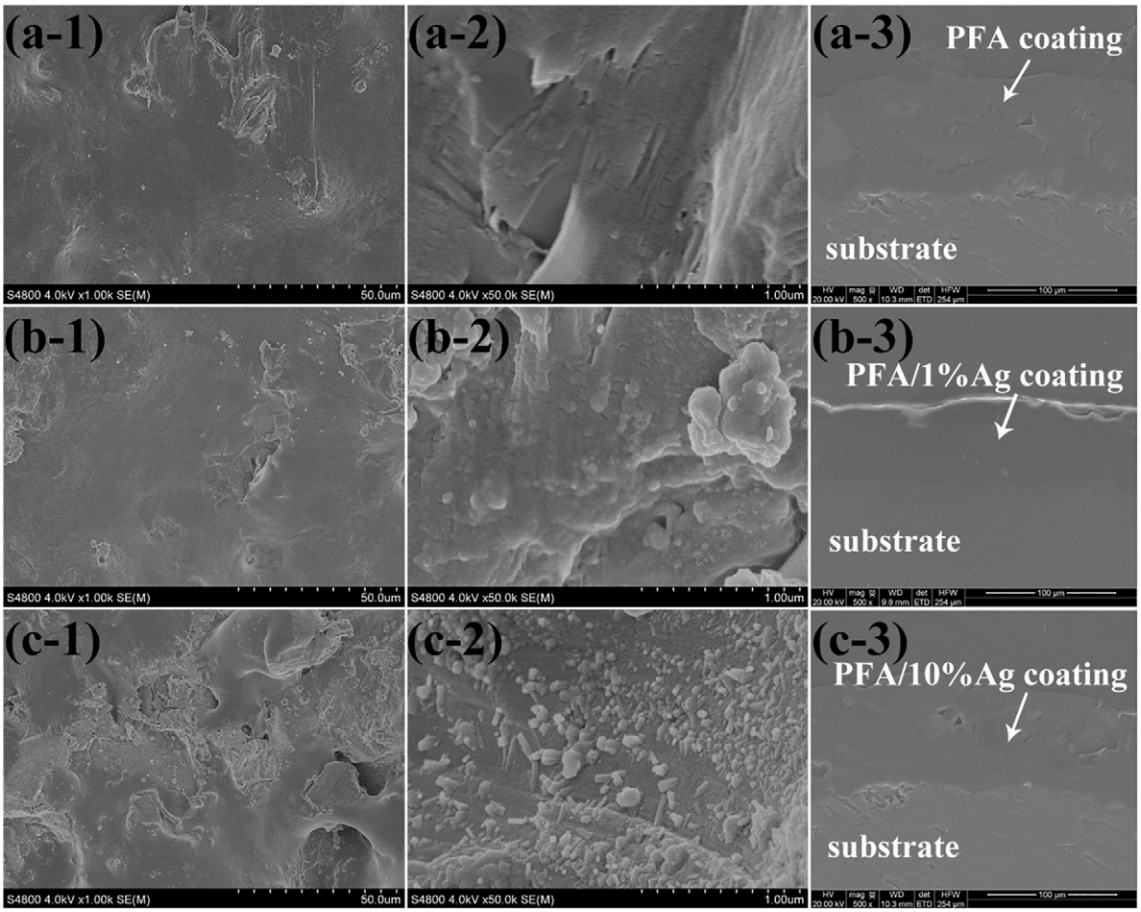

Fig. 1. FE-SEM images of (a) the PFA coating, (b) the PFA/1%Ag coating, and (c) the PFA/10%Ag coating. (-2 is enlarged view of selected area in -1, -3 is cross-sectional view of the coating).

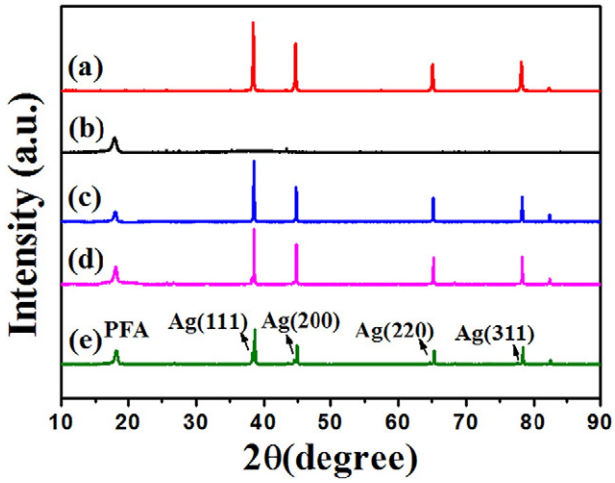

Fig. 2. XRD curves of (a) the aluminum substrate, (b) the PFA powder, (c) the PFA coating, (d) the PFA/1%Ag coating, and (e) the PFA/10%Ag coating.

(DR) rates of the samples were calculated according to the equation:

$$\mathrm{DR}\ (\%) = \frac{C_{\mathrm{uncoated}} - C_{\mathrm{coated}}}{C_{\mathrm{uncoated}}} \times 100$$

where DR is the drag reduction rate; C_{uncoated} is the drag coefficient of the uncoated aluminum substrate; and C_{coated} is the drag coefficient of the coated aluminum substrate.

3. Results and discussion

The PFA coatings with the thickness of ~80 μm show relatively smooth topographical morphology and dense (Fig. 1). For PFA/1%Ag coating, similar surface feature was observed compared to the PFA coating. Nevertheless, a few Ag nanoparticles were found within the PFA coating (Fig. 1b-2). The loading of Ag nanoparticles within PFA coating was achieved by decomposing of $AgNO_3$ during the process of suspension flame spraying at a relatively high temperature. This result is consistent with the result reported in a previous study [34]. The surface of PFA/10%Ag coating (Fig. 1c-1 and c-2) shows much rougher than those of the PFA coating and the PFA/1%Ag coating. Furthermore, it is noteworthy that the quantity and the size of the Ag nanoparticles within the PFA/10%Ag coating was significantly increased (Fig. 1c-2). This phenomenon could be attributed to the high content of silver in the

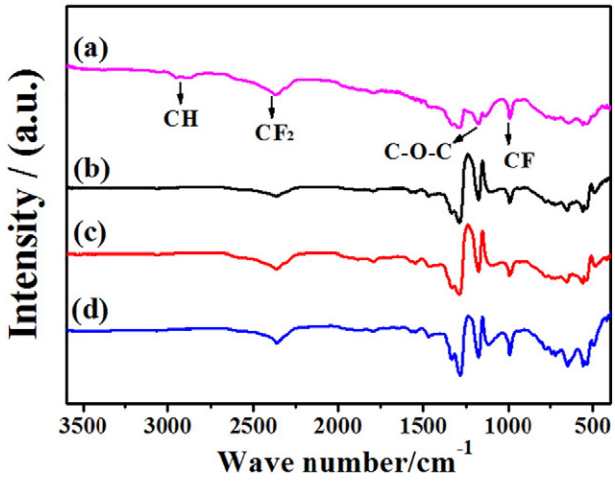

Fig. 3. FTIR spectra of (a) the PFA powder, (b) the PFA coating, (c) the PFA/1%Ag coating, and (d) the PFA/10%Ag coating.

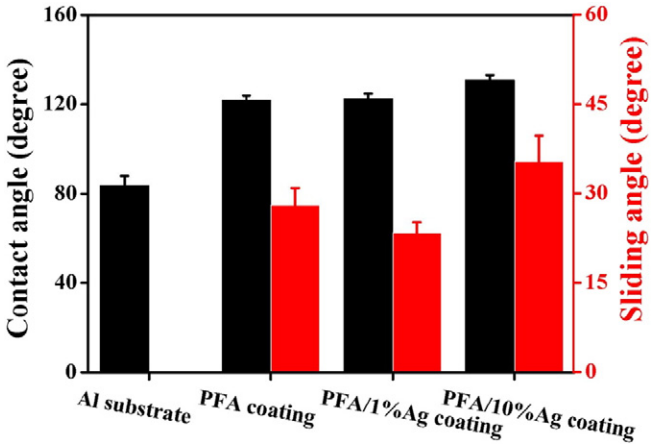

Fig. 4. Water contact angle and sliding angle of the samples.

starting suspension. The result suggests that the PFA/nano-Ag coatings were successfully fabricated.

XRD characterization (Fig. 2) of the overall coatings exhibits the major component as Al due to the relatively thin thickness of the coatings in this study. The PFA coating displays a major component as PFA, indicating the unique advantages of better control over the chemistry of the PFA powder during the suspension flame spraying. The peaks at 38.1°, 44.3°, 64.5°, 77.5° and 81.5° corresponding to the individual crystallographic indices (111), (200), (220) and (311) of the Ag nanoparticles [35] were observed in the XRD pattern of the PFA/1%Ag coating and the PFA/10%Ag coating. The result is consistent with that of SEM as mentioned above (Fig. 1). The result indicates the successful fabrication of the silver nanoparticles-loaded PFA coatings with well retained structure of PFA.

FTIR measurement was performed to further confirm the successful fabrication of the PFA-based coatings (Fig. 3). The overall coatings show almost the same peaks with those of the starting PFA powder. The peak at 1176 cm^{-1} represents the stretching vibration of the C—F present in PFA molecule. The peak at 2365 cm^{-1} is assigned to the combination peak of the two modes associated with the CF_2 backbone. The broad IR peaks located at 2800–2900 cm^{-1} and 2900–3000 cm^{-1} refer to the —CH symmetric and asymmetric stretching of the aliphatic groups in PFA molecule. The peaks at 1288 cm^{-1} and 1176 cm^{-1} are ascribed to stretching vibration of C—O—C [36]. The result once again suggested that the PFA-based coatings were successfully fabricated.

Wettability assessment (Fig. 4) shows hydrophilic characteristics of the aluminum substrates with the CA of ~84°. After the further deposition of the PFA alone by suspension flame spraying on the aluminum substrates, the substrates exhibit the feature of hydrophobicity with the CA of ~121° and SA of ~28°. This is likely due to the hydrophobic nature of the PFA [37–40]. It is noted that the CA slightly increased from 121° to 123° after the silver nanoparticles loaded. In addition, the PFA/1%Ag coatings show a SA of ~23°, more slippery than PFA coatings. Synergistic effect of the PFA and the silver nanoparticles is suggested for the lower SA. It is believed that apart from surface chemistry, surface roughness plays important roles in accomplishing the hydrophobicity [41]. The PFA/10%Ag coatings display excellent hydrophobic property with the CA of ~135°. Surprisingly, the SA of the PFA/10%Ag coatings significantly increased, with the SA of ~33°. This might be due to the fact that

Table 1
Cumulative release of silver from different samples (mg/L).

Samples	7 days	21 days
PFA/1%Ag coating	/	0.05
PFA/10%Ag coating	/	5

/: below the detection limit.

the structures such as that shown in Fig. 1c cannot trap sufficient air in the structure for low sliding angles [42].

Sustained release of antifoulant from the coatings is of particular importance for their long-term marine antifouling applications. Table 1 shows the cumulative release of silver from the samples after immersion in NaCl solution for 7 and 21 days, respectively. The concentration of silver ions released from both the PFA/1%Ag coatings and the PFA/10%Ag coatings is below the detection limit after 7 days of immersion. The phenomenon could be interpreted that the releasing rate of silver ions was inhibited by the PFA molecules due to its hydrophobic nature. Significant amount of silver ions were detected after 21 days immersion at the level of 0.05 mg/L and 5 mg/L for the PFA/1%Ag coatings and PFA/10%Ag coatings, respectively. The result implies that the approach presents here has potential applications for the development of PFA-based control release coatings with long-term antifouling property.

After 24 h incubation in ASW, the aluminum substrates and the PFA coatings exhibit clear adhesion of *E. coli* (Fig. 5a and b). The presence of PFA coating reduces the affinity of the bacteria on the surfaces of the PFA layer coated aluminum substrates. This indicates the effect of the hydrophobic property of the PFA coatings on adhesion of the bacteria. The result is consistent with previous studies [43,44]. No bacteria could be observed on the surfaces of the PFA/1%Ag coatings (Fig. 5c). Similar result was obtained for the PFA/10%Ag coatings (Fig. 5d). It is noteworthy that the silver ion released from both the PFA/1%Ag coatings and the PFA/10%Ag coatings is below the minimum inhibitory concentration (MIC) of silver ions for *E. coli* [45]. This phenomenon might be related to the fact that contact killing [46,47] is the predominant antimicrobial mechanism and surfaces immobilized silver nanoparticles exhibit better efficacy than those of surfaces that released silver ions only. The result is similar to a previous study reported for similar surface immobilized silver nanoparticles [48]. Thus, we demonstrate that contact killing and ion mediated killing of silver nanoparticles and hydrophobic property of the PFA synergistically inhibited the adhesion of *E. coli*. Moreover, the antibacterial properties of the PFA/1%Ag coatings and the PFA/

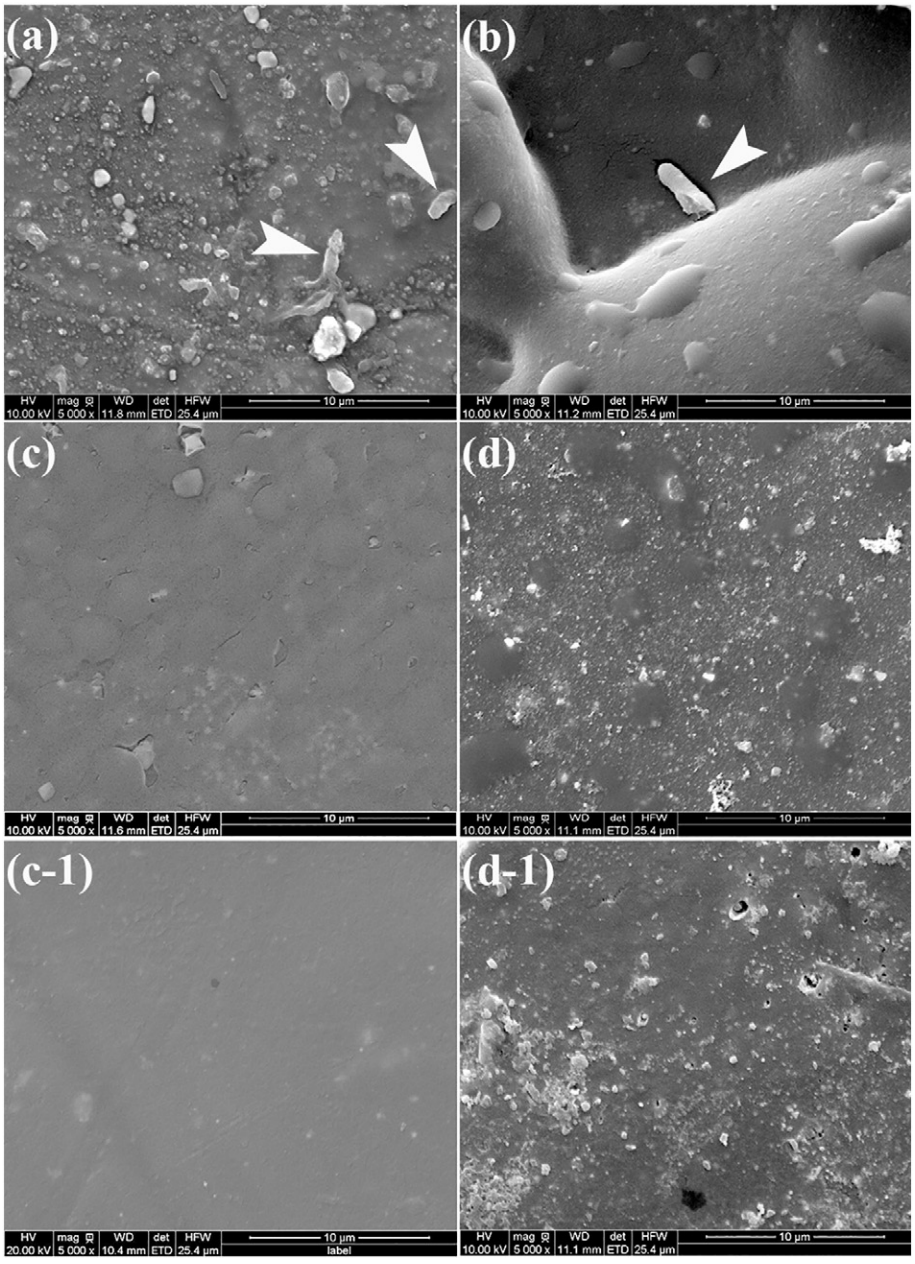

Fig. 5. SEM images of the *E. coli* bacteria attaching on the surfaces of the samples after incubated in *E. coli*-containing suspension for 1 day: (a) the aluminum substrate, (b) the PFA coating, (c) the PFA/1%Ag coating, and (d) the PFA/10%Ag coating. (−1 is the samples after incubated in *E. coli*-containing suspension for 21 days).

10%Ag coatings were constant even the samples incubated in ASW for 21 days, since the releasing rate of silver ions was inhibited by the hydrophobic PFA (Fig. 5c-1 and d-1). Thus, this study presents an alternative for the fabrication of surface functionalized marine metal with long-term antifouling property.

To investigate the feasibility of the present approach for the large-scale development of hydrophobic coatings, hydrophobic PFA-based coatings were deposited on aluminum plates with the dimension of 200 mm × 300 mm × 11.2 mm. Drag reduction tests were performed on the abovementioned samples. Fig. 6 shows the drag coefficients (C_f) of the aluminum substrate and the aluminum substrates with PFA-based coatings obtained in a relatively wide flow velocity range, from 5 m/s to 11 m/s. In addition, to show the measured results more quantitatively, the drag reduction rates (DR) of the coated surfaces were also shown in Table 2. As seen from the result, the drag coefficients of the uncoated substrate decreased when the flow velocity increased. However, completely different results were obtained for the coated samples. This tendency could be associated to the fact that the drag effect resulting from wave contribution becomes dominant relatively to the frictional drag contribution [49]. In addition, the drag coefficients of the PFA coated substrate is slightly lower than that of the uncoated aluminum substrate at a flow velocity of 5 m/s, showing a drag reduction rate of 5%. However, the drag coefficient of the PFA coating is higher than that of the uncoated surface at higher flow velocity, indicating an unavoidable failure of drag reduction. The drag coefficient of the PFA/1%Ag coating is lower than that of the uncoated aluminum substrate at a relatively low flow velocity of 5 m/s, showing a drag reduction rate of 28%. It is still lower than that of the uncoated aluminum substrate at a flow velocity of 8 m/s, showing a drag reduction rate of 11%. However, the drag coefficients of the PFA/1%Ag coating presents slightly higher than that of the uncoated aluminum substrate at a high flow velocity of 11 m/s. Nevertheless, the result suggests obvious drag reduction between the uncoated substrate and PFA/1%Ag coating. This drag-reducing effect is similarly observed on traditional hydrophobic surfaces. When hydrophobic surfaces are tested at high wall shear rates, the surfaces do not show a significant drag reduction effect. It is interesting that the drag coefficient of the PFA/10%Ag coating is much higher than those of the overall other samples, showing a significant increase of drag. This could be associated to the increased roughness of the PFA/10%Ag coating, since the dominant factor affecting drag performance is known to be the surface roughness. Moreover, the adhesion of marine biofouling onto the surfaces without good antifouling properties would further increase the roughness of the surfaces. Our ongoing efforts are therefore being devoted to elucidating the relation between the antifouling and drag performance. Taken together, we confirmed our hypothesis that silver-loaded PFA coatings (PFA/1%Ag coating) exhibit both antifouling and drag-reducing effect. Furthermore, the proposed method to fabricate antifoulant-loaded hydrophobic PFA coatings has many advantages, such as large-area fabrication, universal applicability, a simple procedure, and low cost. Nevertheless, the loading amount of Ag should be optimized for practical applications.

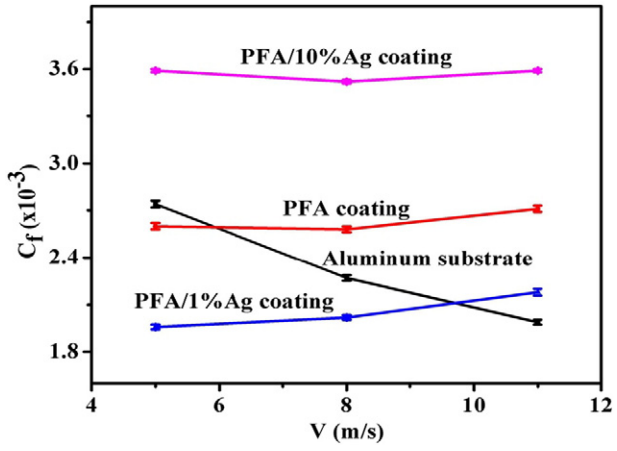

Fig. 6. Drag measurement results on the PFA/10%Ag coating, the aluminum substrate, the PFA coating, and the PFA/1%Ag coating.

Table 2
Result of drag coefficient (C_f) and drag reduction rate (DR) of the samples. PFA: PFA coating; PFA1: PFA/1%Ag coating; PFA10: PFA/10%Ag coating.

V	5 m/s			8 m/s			11 m/s		
Type	PFA	PFA1	PFA10	PFA	PFA1	PFA10	PFA	PFA1	PFA10
C_f	2.60	1.96	3.59	2.58	2.02	3.52	2.71	2.18	3.59
DR	5%	28%	−30%	−14%	11%	−55%	−30%	−10%	−80%

4. Conclusions

In this study, we fabricated antifoulant-loaded hydrophobic PFA coatings with silver nanoparticles by suspension flame spraying. SEM, XRD, FTIR and water contact angle measurements demonstrated that PFA/nano-Ag composite coatings were successfully constructed. The coatings containing 1%Ag show more slippery, remarkable enhanced antifouling and drag reduction properties. The study gives insight into antifouling and drag reduction applications of antifoulant-loaded hydrophobic coatings for marine vehicles.

Acknowledgement

This work was supported by CAS-Iranian Vice Presidency for Science and Technology Joint Research Project (grant # 174433KYSB20160085), National Natural Science Foundation of China (grant # 51401232), and Ningbo Municipal Major Projects on Industrial Technology Innovation (grant # 2015B11054).

References

[1] K. Yin, X.R. Dong, F. Zhang, C. Wang, J. Duan, Superamphiphobic miniature boat fabricated by laser micromachining, Appl. Phys. Lett. 110 (2017) 121909.
[2] D.M. Yebra, S. Kiil, K. Dam-Johansen, Antifouling technology — past, present and future steps towards efficient and environmentally friendly antifouling coatings, Prog. Org. Coat. 50 (2004) 75–104.
[3] A.V. Tulcidas, R. Bayon, A. Igartua, J.C.M. Bordado, E.R. Silva, Friction reduction on recent non-releasing biocidal coatings by a newly designed friction test rig, Tribol. Int. 91 (2015) 140–150.
[4] X.Q. Bai, G.T. Xie, H. Fan, Z.X. Peng, C.Q. Yuan, X.P. Yan, Study on biomimetic preparation of shell surface microstructure for ship antifouling, Wear 306 (2013) 285–295.
[5] W.E.G. Mueller, X. Wang, Y.W. Guo, H.C. Schroeder, Potentiation of the cytotoxic activity of copper by polyphosphate on biofilm-producing bacteria: a bioinspired spproach, Mar. Drugs 10 (2012) 2369–2387.
[6] W.E.G. Mueller, X. Wang, P. Proksch, C.C. Perry, R. Osinga, J. Garderes, H.C. Schroeder, Principles of biofouling protection in marine sponges: a model for the design of novel biomimetic and bio-inspired coatings in the marine environment? Mar. Biotechnol. 15 (2013) 375–398.
[7] G.D. Bixler, B. Bhushan, Biofouling: lessons from nature, Philos. T. R. Soc. A 370 (2012) 2381–2417.
[8] R.L. Townsin, The ship hull fouling penalty, Biofouling 19 (2003) 9–15.
[9] K.P. Logan, Using a ship's propeller for hull condition monitoring, Nav. Eng. J. 124 (2012) 71–87.
[10] Y. Liu, P. Guo, X. He, L. Li, A. Wang, H. Li, Developing transparent copper-doped diamond-like carbon films for marine antifouling applications, Diam. Relat. Mater. 69 (2016) 144–151.
[11] Q. Yu, W.Y. Ge, A. Atewologun, A.D. Stiff-Roberts, G.P. Lopez, Antimicrobial and bacteria-releasing multifunctional surfaces: oligo (p-phenylene-ethynylene)/ poly (N-isopropylacrylamide) films deposited by RIR-MAPLE, Colloid. Surface. B 126 (2015) 328–334.
[12] X. Bai, X. Zhang, C. Yuan, Numerical analysis of drag reduction performance of different shaped riblet surfaces, Mar. Technol. Soc. J. 50 (2016) 62–72.
[13] K.G. Krishnan, A. Milionis, E. Loth, T.E. Farrell, J.D. Crouch, D.H. Berry, Influence of hydrophobic and superhydrophobic surfaces on reducing aerodynamic insect residues, Appl. Surf. Sci. 392 (2017) 723–731.
[14] S. Martin, B. Bhushan, Modeling and optimization of shark-inspired riblet geometries for low drag applications, J. Colloid Interface Sci. 474 (2016) 206–215.
[15] B.G. Paik, K.Y. Kim, S.R. Cho, J.W. Ahn, S.R. Cho, Investigation on drag performance of anti-fouling painted flat plates in a cavitation tunnel, Ocean Eng. 101 (2015) 264–274.

[16] M. Ferrari, A. Benedetti, Superhydrophobic surfaces for applications in seawater, Adv. Colloid Interf. Sci. 222 (2015) 291–304.
[17] G.D. Bixler, B. Bhushan, Rice and butterfly wing effect inspired low drag and antifouling surfaces: a review, Crit. Rev. Solid State 40 (2015) 1–37.
[18] K. Liu, Y. Tian, L. Jiang, Bio-inspired superoleophobic and smart materials: design, fabrication, and application, Prog. Mater. Sci. 58 (2013) 503–564.
[19] X. Chen, Y. Gong, D. Li, H. Li, Robust and easy-repairable superhydrophobic surfaces with multiple length-scale topography constructed by thermal spray route, Colloid. Surface. A 492 (2016) 19–25.
[20] X. Chen, J. Yuan, J. Huang, K. Ren, Y. Liu, S. Lu, H. Li, Large-scale fabrication of superhydrophobic polyurethane/nano-Al_2O_3 coatings by suspension flame spraying for anti-corrosion applications, Appl. Surf. Sci. 311 (2014) 864–869.
[21] P. Qian, L. Chen, Y. Xu, Mini-review: molecular mechanisms of antifouling compounds, Biofouling 29 (2013) 381–400.
[22] I. Sondi, B. Salopek-Sondi, Silver nanoparticles as antimicrobial agent: a case study on *E. coli* as a model for Gram-negative bacteria, J. Colloid Interface Sci. 275 (2004) 177–182.
[23] M. Gopiraman, A.W. Jatoi, S. Hiromichi, K. Yamaguchi, H.Y. Jeon, I.M. Chung, I.S. Kim, Silver coated anionic cellulose nanofiber composites for an efficient antimicrobial activity, Carbohydr. Polym. 149 (2016) 51–59.
[24] Y.S. Wei, K.S. Chen, L.T. Wu, In situ synthesis of high swell ratio polyacrylic acid/silver nanocomposite hydrogels and their antimicrobial properties, J. Inorg. Biochem. 164 (2016) 17–25.
[25] X. Zhang, X. Wang, D. Wu, Design and synthesis of multifunctional microencapsulated phase change materials with silver/silica double-layered shell for thermal energy storage, electrical conduction and antimicrobial effectiveness, Energy 111 (2016) 498–512.
[26] N.J. Shikuma, M.G. Hadfield, Marine biofilms on submerged surfaces are a reservoir for *Escherichia coli* and *Vibrio cholerae*, Biofouling 26 (2010) 39–46.
[27] S. Dobretsov, M. Teplitski, V. Paul, Mini-review: quorum sensing in the marine environment and its relationship to biofouling, Biofouling 25 (2009) 413–427.
[28] S. Dobretsov, M. Teplitski, M. Bayer, S. Gunasekera, P. Proksch, V.J. Paul, Inhibition of marine biofouling by bacterial quorum sensing inhibitors, Biofouling 27 (2011) 893–905.
[29] X. He, Y. Liu, J. Huang, X. Chen, K. Ren, H. Li, Adsorption of alginate and albumin on aluminum coatings inhibits adhesion of *Escherichia coli* and enhances the anti-corrosion performances of the coatings, Appl. Surf. Sci. 332 (2015) 89–96.
[30] P. Zhu, W. Meng, Y. Huang, Synthesis and antibiofouling properties of crosslinkable copolymers grafted with fluorinated aromatic side chains, RSC Adv. 7 (2017) 3179–3189.
[31] G. Xu, D. Pranantyo, B. Zhang, L. Xu, K.G. Neoh, E.T. Kang, Tannic acid anchored layer-by-layer covalent deposition of parasin I peptide for antifouling and antimicrobial coatings, RSC Adv. 6 (2016) 14809–14818.
[32] R.F.M. Elshaarawy, F.H.A. Mustafa, A. Herbst, A.E.M. Farag, C. Janiak, Surface functionalization of chitosan isolated from shrimp shells, using salicylaldehyde ionic liquids in exploration for novel economic and ecofriendly antibiofoulants, RSC Adv. 6 (2016) 20901–20915.
[33] F. Maia, A.P. Silva, S. Fernandes, A. Cunha, A. Almeida, J. Tedim, M.L. Zheludkevich, M.G.S. Ferreira, Incorporation of biocides in nanocapsules for protective coatings used in maritime applications, Chem. Eng. J. 270 (2015) 150–157.
[34] D.Q. Xu, Y.L. Su, L.L. Zhao, F.C. Meng, C. Liu, Y.Y. Guan, J.Y. Zhang, J.B. Luo, Antibacterial and antifouling properties of a polyurethane surface modified with perfluoroalkyl and silver nanoparticles, J. Biomed. Mater. Res. A 105 (2017) 531–538.
[35] M. Aliabadi, One-step synthesis of highly efficient TiO_2-CdS-Ag nanocomposite for remove organic pollution, Sep. Purif. Technol. 174 (2017) 145–149.
[36] M.A. Sidebottom, A.A. Pitenis, C.P. Junk, D.J. Kasprzak, G.S. Blackman, H.E. Burch, K.L. Harris, W.G. Sawyer, B.A. Krick, Ultralow wear perfluoroalkoxy (PFA) and alumina composites, Wear 362-363 (2016) 179–185.
[37] K. Li, X. Zeng, H. Li, X. Lai, Fabrication and characterization of stable superhydrophobic fluorinated-polyacrylate/silica hybrid coating, Appl. Surf. Sci. 298 (2014) 214–220.
[38] Y. Zhang, A.L. Yarin, Carbon nanofibers decorated with poly(furfuryl alcohol)-derived carbon nanoparticles and tetraethylorthosilicate-derived silica nanoparticles, Langmuir 27 (2011) 14627–14631.
[39] K.W. Wang, N.X. Hu, G. Xu, Y. Qi, Stable superhydrophobic composite coatings made from an aqueous dispersion of carbon nanotubes and a fluoropolymer, Carbon 49 (2011) 1769–1774.
[40] M. Doms, H. Feindt, W.J. Kuipers, D. Shewtanasoontorn, A.S. Matar, S. Brinkhues, R.H. Welton, J. Mueller, Hydrophobic coatings for MEMS applications, J. Micromech. Microeng. 18 (2008), 055030.
[41] X. Chen, Y. Gong, X. Suo, J. Huang, Y. Liu, H. Li, Construction of mechanically durable superhydrophobic surfaces by thermal spray deposition and further surface modification, Appl. Surf. Sci. 356 (2015) 639–644.
[42] M. Miwa, A. Nakajima, A. Fujishima, K. Hashimoto, T. Watanabe, Effects of the surface roughness on sliding angles of water droplets on superhydrophobic surfaces, Langmuir 16 (2000) 5754–5760.
[43] J.S. Chung, B.G. Kim, S. Shim, S.E. Kim, E.H. Sohn, J. Yoon, J.C. Lee, Silver-perfluorodecanethiolate complexes having superhydrophobic, antifouling, antibacterial properties, J. Colloid Interface Sci. 366 (2012) 64–69.
[44] C.H. Xue, X.J. Guo, J.Z. Ma, S.T. Jia, Fabrication of robust and antifouling superhydrophobic surfaces via surface-initiated atom transfer radical polymerization, ACS Appl. Mater. Interfaces 7 (2015) 8251–8259.
[45] M.A. Radzig, V.A. Nadtochenko, O.A. Koksharova, J. Kiwi, V.A. Lipasova, I.A. Khmel, Antibacterial effects of silver nanoparticles on gram-negative bacteria: influence on the growth and biofilms formation, mechanisms of action, Colloid. Surface. B 102 (2013) 300–306.
[46] N. Durán, M. Durán, M.B. de Jesus, A.B. Seabra, W.J. Fávaro, G. Nakazato, Silver nanoparticles: A new view on mechanistic aspects on antimicrobial activity, Nanomedicine: NBM 12 (2016) 789–799.
[47] C.N. Lok, C.M. Ho, R. Chen, Q.Y. He, W.Y. Yu, H. Sun, P.K.H. Tam, J.F. Chiu, C.M. Che, Proteomic analysis of the mode of antibacterial action of silver nanoparticles, J. Proteome Res. 5 (2006) 916–924.
[48] S. Agnihotri, S. Mukherji, S. Mukherji, Immobilized silver nanoparticles enhance contact killing and show highest efficacy: elucidation of the mechanism of bactericidal action of silver, Nano 5 (2013) 7328–7340.
[49] B.W. Song, F. Ren, H.B. Hu, Y.H. Guo, Drag reduction on micro-structured hydrophobic surfaces due to surface tension effect, Acta Phys. Sin. 63 (2014), 054708.